NASA TECHNICAL NOTE

NASA TN D-2276

C.1

LOAN COPY:
AFWL
KIRTLAND

0154973

TECH LIBRARY KAFB, NM

NASA TN D-2276

EXPERIMENTAL DETERMINATION OF SODIUM VAPOR EXPANSION CHARACTERISTICS WITH INERT-GAS-INJECTION PRESSURE-MEASURING TECHNIQUE

by Landon R. Nichols, Stanley M. Nosek, Charles H. Winzig, and Louis J. Goldman

Lewis Research Center
Cleveland, Ohio

NATIONAL AERONAUTICS AND SPACE ADMINISTRATION • WASHINGTON, D. C. • APRIL 1964

TECH LIBRARY KAFB, NM
0154973

EXPERIMENTAL DETERMINATION OF SODIUM VAPOR EXPANSION CHARACTERISTICS WITH INERT-GAS-INJECTION PRESSURE-MEASURING TECHNIQUE

By Landon R. Nichols, Stanley M. Nosek, Charles H. Winzig, and Louis J. Goldman

Lewis Research Center
Cleveland, Ohio

NATIONAL AERONAUTICS AND SPACE ADMINISTRATION

For sale by the Office of Technical Services, Department of Commerce, Washington, D.C. 20230 -- Price $1.00

EXPERIMENTAL DETERMINATION OF SODIUM VAPOR EXPANSION CHARACTERISTICS WITH INERT-GAS-INJECTION PRESSURE-MEASURING TECHNIQUE

by Landon R. Nichols, Stanley M. Nosek, Charles H. Winzig, and Louis J. Goldman

Lewis Research Center

SUMMARY

An inert-gas-injection technique was successfully used to measure accurately the static pressures of vaporous sodium expanding through an axisymmetrical convergent-divergent nozzle. Wall-pressure and axial-pressure profiles through the nozzle were determined. A search probe was actuated axially through the nozzle with a bellows seal to separate the sodium from the atmosphere.

The research nozzle was 3.75 inches long with an inlet diameter of 3 inches and an outlet diameter of 0.845 inch. The throat of the nozzle had a diameter of 0.677 inch and was located 2.52 inches from the nozzle inlet. The nozzle inlet pressure was varied from approximately 6 to 29 inches of mercury absolute; the inlet temperature ranged from 1380° to 1650° F, and vapors with indicated superheat up to 60° F were studied. The receiving pressure was varied to allow essentially complete expansion through the supersonic nozzle.

Comparison of the experimentally determined expansion characteristics of the metallic vapors with a theoretical one-dimensional isentropic expansion of a gas indicated that an expansion index n of 1.3 (from the law $pv^n = c$, where p is absolute pressure, v is specific volume, and c is a constant) best represented the experimental data over the range of nozzle inlet conditions investigated.

Further study at higher levels of superheat are recommended to substantiate results.

INTRODUCTION

The application of alkali metals as working fluids for space power Rankine systems has emphasized the need for accurate and more extensive knowledge of their physical and thermodynamic properties. This knowledge is essential to

evaluate properly the processes, such as vaporization, expansion, and condensation, that occur in this cycle. The vapor phase is of particular concern because its properties are complicated by molecular weight changes due to polymerization reaction and also, because it is a condensible, by changes in phase. The proper design of turbines is, therefore, of particular concern because under the rapidly expanding flow conditions in a turbine these changes are difficult to predict.

Currently, there are two choices usually considered for the process on which to base the design of a turbine. One is the equilibrium expansion process, in which the expansion is assumed to occur with equilibrium both between physical phases of vapor and liquid and between chemical reaction species of monatomic and diatomic molecules. The second choice is a supersaturated expansion process, which in references 1 and 2 is indicated as perhaps more plausible, at least for sodium vapor. In this process, it is assumed that condensation is delayed so that the fluid remains vaporous throughout the expansion. It is also assumed that the expansion proceeds too rapidly to allow any change in the chemical equilibrium from the initial state point. The vapor is presumed to behave as an ideal gas, and the ratio of the specific heat at constant pressure to the specific heat at constant volume is taken as the index n in the law $pv^n = c$ for the expansion process. (Symbols are defined in appendix A.) The theoretically calculated performance between the two processes is significantly different; consequently, a more accurate identification of the expansion process is required. Thermodynamic-property data may be taken from references such as reference 3, a comprehensive compilation for most alkali metals, or reference 4, which is specifically for sodium.

The purpose of the investigation reported herein was to determine the expansion process index for saturated and superheated sodium vapor. The pressure distribution of the sodium vapor expanding through a convergent-divergent nozzle was to be measured, and the results were then to be compared with the pressure distribution theoretically calculated for a gas expanding isentropically. The accurate pressure measurements necessary for this purpose were to be attempted by the use of an inert-gas-injection technique. By this method, the sodium process pressure is null balanced with an inert gas barrier so that readings could be taken with a mercury manometer.

The nozzle inlet pressure was varied from approximately 6 to 29 inches of mercury absolute, and the receiving or condenser pressure was varied from 1 to 7 inches of mercury absolute to provide supersonic flow through the nozzle. Heat was added to the vapors leaving the liquid-vapor separator in an attempt to evaporate any entrained droplets and thus obtain dry vapors into the nozzle. Vapors, with up to 60° F indicated superheat, were used.

In addition to pressure measurements along the wall of the nozzle, the static pressure along the axis of the nozzle was also measured with a bellows-sealed traversing probe. The probe was also used to detect signs of condensation by providing measurements over small increments of travel.

EQUIPMENT

Vapor-Generation System

The investigation covered by this report was conducted in a sodium flash-vaporization facility. A detailed discussion of the facility and the generation of sodium vapor is given in reference 2. To carry out the research reported herein, the facility was modified by replacement of the simple convergent nozzle and the environmental chamber with a convergent-divergent nozzle research assembly. Heaters were added to the 3-inch vapor line for superheating the vapor from the separator to the nozzle. A brief discussion of the process scheme of the facility will be given here with reference to figure 1, which indicates the major components and peak design parameters.

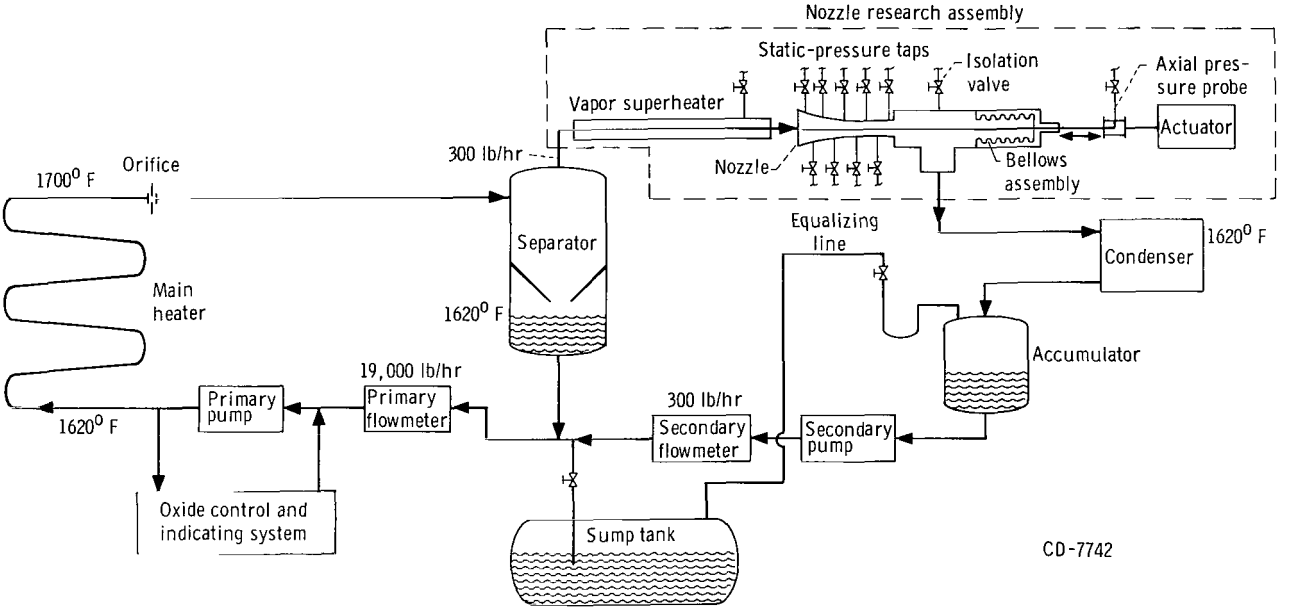

Figure 1. - Schematic drawing of sodium flash-vaporization facility.

Saturated liquid at temperatures as high as 1620° F and at flow rates up to 50 gallons per minute (19,000 lb/hr) is circulated by an electromagnetic pump from a liquid-vapor separator to the main heater. The compressed liquid is heated to 1700° F in the electrical-resistance heater. Decompression of the liquid due to flow through an orifice located at the outlet of the heater allows fractional vaporization. The two-phase mixture is separated in a centrifugal separator. The liquid portion passes out of the bottom and returns to the pump. In parallel with the pump is an oxide control and indicating system to maintain and monitor the purity of the molten sodium.

Vapor at rates up to 300 pounds per hour passes from the separator, through the superheater, the convergent-divergent nozzle, and then to an air-cooled condenser. The saturated condensate enters an accumulator from which it flows through the secondary pump and flowmeter before combining with the primary

liquid flow from the separator.

Nozzle Research Assembly

The nozzle research assembly is shown schematically in figure 2 and isometrically in figure 3. The thermodynamic path is shown on the enthalpy-entropy diagram in figure 4 with state points corresponding to those shown in figure 2. The assembly is composed essentially of an axisymmetrical convergent-divergent nozzle with wall static-pressure taps, and a bellows-sealed axial-static-pressure probe.

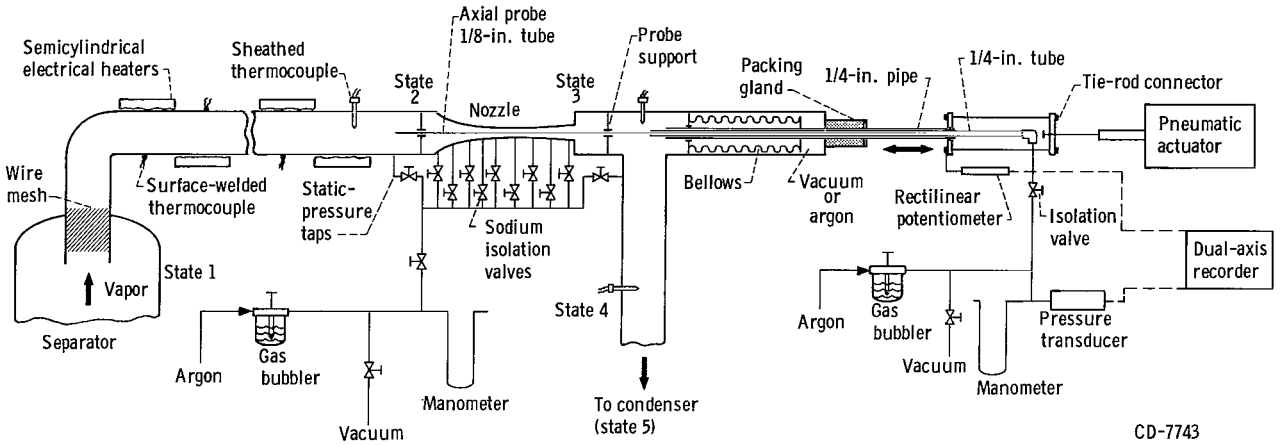

Figure 2. - Schematic drawing of nozzle research assembly.

Nozzle and wall taps. - A schematic diagram of the nozzle is shown in figure 5. The convergent section of the nozzle is elliptical in contour and fairs at about 1/4 inch downstream of the throat into a conical divergent section. The nozzle was machined from 316 stainless steel. After completion of the contour, the nozzle was mounted on a jig boring machine, and diameters at various axial locations were measured. The contour at the throat was flat for 0.030 inch. The throat tap was located at the middle of the flat, and the remaining eight wall taps were then located with the throat tap as reference. The locations of the wall taps and the contour diameters at these locations are listed in figure 5. A 1/8-inch drill was passed perpendicularly from the outside wall of the nozzle to within 0.060 inch of the inside wall of the nozzle. The pressure taps were completed with 0.020-inch burr-free, square-edge holes. A pressure transfer line of 1/4-inch 316 stainless-steel tubing with a 0.095-inch-thick wall connects each tap to a sodium isolation valve.

The inlet to the nozzle has a diameter of 3.06 inches and is welded to the 3-inch vapor pipe at the upstream-strut probe support. The diameter is 0.677 inch at the throat and 0.845 inch at the outlet, while the length from the inlet to the outlet is 3.75 inches. The nozzle is welded to a 3-inch tee at the downstream-strut probe support.

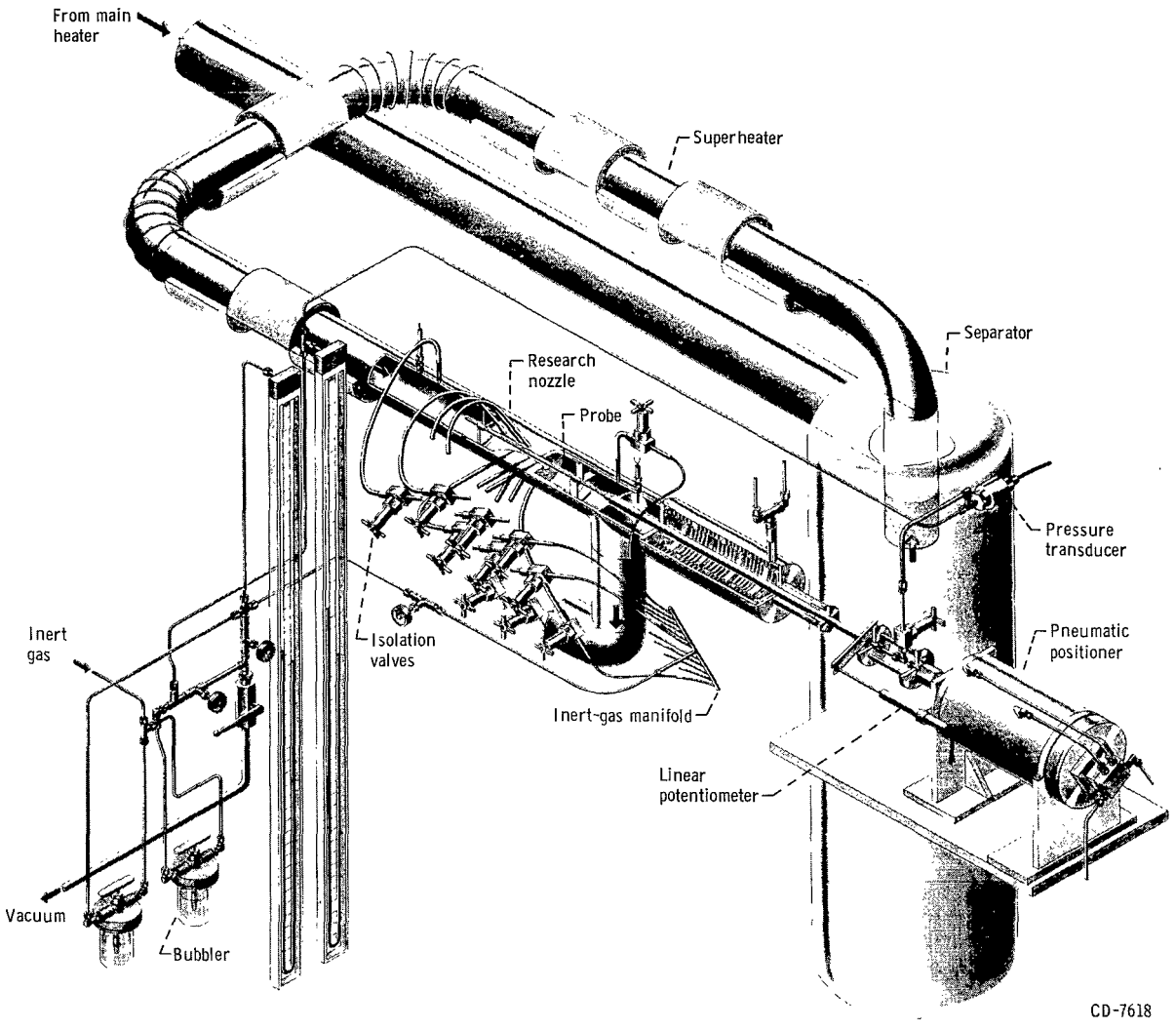

Figure 3. - Research nozzle assembly showing arrangement for inert-gas-pressure measuring technique.

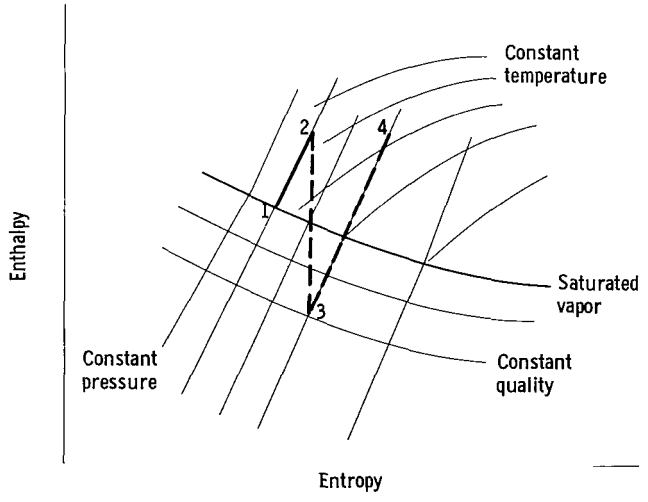

Figure 4. - Thermodynamic path through nozzle research assembly.

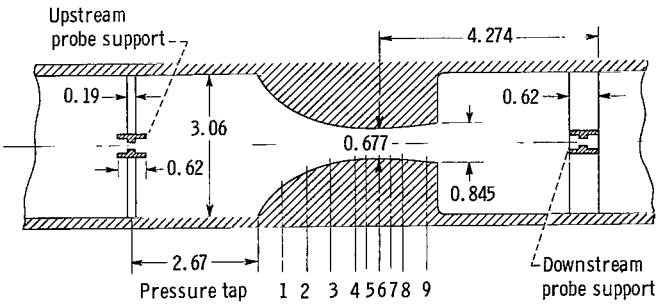

Nozzle diameter at pressure tap locations

Pressure tap	Distance from inlet, in.	Nozzle diameter, in.
1	0.52	1.584
2	1.02	1.129
3	1.52	.866
4	2.02	.721
5	2.27	.689
6 (throat)	2.52	.677
7	2.77	.691
8	3.02	.725
9	3.52	.803

CD-7744

Figure 5. - Diagrammatic sketch and dimensions of nozzle.

A nozzle inlet pressure tap is located 4 inches upstream of the upstream probe support. A receiving or condenser pressure tap is located in the tee downstream of the nozzle.

Axial-pressure probe. - Drawings of the axial-pressure probe and bellows seal are included in figures 2 and 3. The probe is 1/8-inch tubing that is 42 inches long and has a wall thickness of 0.018 inch.

Struts at either end of the nozzle as shown in figures 2, 3, and 5 support and guide the probe along the axis of the nozzle. Stellite inserts are used as bearings to prevent self-welding to the probe, and a sliding clearance of 0.003 inch is provided.

The upstream end of the probe is closed off with a tapered plug. The portion passing through the tee and bellows assembly is enclosed in a 28-inch length of 1/4-inch tubing. The annulus at the ends of the two tubes is welded shut, and the end is connected to a 1/4-inch bellows-sealed sodium isolation valve. Four 0.020-inch static pressure sensing holes, spaced 90° apart radially, are located in the probe 6.685 inches from the left end of the 1/4-inch tube. With the 1/4-inch tube against the downstream probe support as a stop and position reference, the sensing holes are at the inlet of the nozzle. The distance from the strut to the throat wall tap was measured (see fig. 5); therefore, as the 1/4-inch tube traveled away from the strut, the travel and exact location of the probe relative to the nozzle could be readily determined.

The probe together with the 1/4-inch tube are driven by the bellows-sealed 1/4-inch pipe through which they pass. The right end of this pipe terminates at the tie-rod connector and is closed around the 1/4-inch tube. The left end terminates in the 3-inch tee, which serves to connect the nozzle, the bellows assembly, and the condenser.

The composite bellows was fabricated from four single-ply 0.005-inch stainless-steel bellows with an outside diameter of $3\frac{31}{32}$ inches and an inside diameter of 3 inches. Each of the bellows sections has nine corrugations. The sections were joined with connector rings by furnace brazing in a reducing atmosphere. The right end of the composite bellows was brazed to a stainless-steel disk, which was welded to the 1/4-inch pipe. The left end of the bellows

was brazed to a ring, which was welded to a support disk. The bellows housing is welded to the same disk, and the disk is, in turn, welded to the tee. A hole through the center of the disk provides passage and support for the 1/4-inch pipe containing the probe. A hole at the bottom of the disk allows free drainage of sodium from the bellows chamber into the tee.

The bellows housing is an 11-inch length of 4-inch pipe with the inside surface smoothly finished. The right end of the housing contains a conventional packing gland to support the 1/4-inch pipe and to seal the housing. The packing was made with asbestos string, lubricated with molybdenum disulfide. The bellows housing was equipped with vacuum and argon services to control the pressure differential across the bellows. When the probe was not being operated, this differential was maintained at a minimum to prolong the life of the bellows. When the probe was in operation, the differential was increased sufficiently to allow the probe to move in (upstream). The pneumatic drive mechanism was utilized to control the motion and the position. The probe was moved out (downstream) entirely by the pneumatic drive with no assistance from pressure differential across the bellows.

Pressure-measuring techniques. - The 11 wall pressure taps, that is, the nozzle inlet pressure tap, the nozzle pressure taps, and the receiving pressure tap, were joined to a common manifold (fig. 2). Line heaters were used to sustain the pressure transfer lines (connecting the wall taps to the respective isolation valves) and the isolation valves at 250° to 400° F when pressure measurements were being taken. With the desired nozzle inlet conditions and the desired receiving pressure set, the manifold and the U-tube mercury-filled manometer are pressurized with argon to a few inches of mercury greater than the nozzle inlet pressure as determined by the vapor pressure in the separator. The argon is introduced through a visual glass-bowl bubbler partly filled with mineral oil.

The wall pressures were generally taken in sequence beginning with the farthest upstream or nozzle inlet pressure tap. The appropriate sodium isolation valve is opened to permit the flow of argon into the nozzle. The inert-gas pressure null balances the pressure of the sodium vapor as indicated by no further change in the mercury column. Pressure measurements taken both with gas flow, as indicated by the visual bubbler, and without gas flow showed no difference in the measured pressure if the gas flow did not exceed about 8 cubic centimeters per minute at the pressure existing in the manifold system. Frequent random checks showed no differences in the measured pressure. Sequential measurements are desirable to reduce the amount of inert gas injected into the process system. A manifold inert-gas pressure, a few inches of mercury greater than the predicted system pressure, is needed initially to force any condensed sodium between the isolation valve and the 0.020-inch wall tap into the flowing sodium vapor stream.

Axial-pressure-probe measurements were also made with the inert-gas null-balance technique. The probe was also equipped with a sodium isolation valve. The axial probe and the pressure transfer line up to and including the valve were heated with electrical-resistance heaters and heating lamps when pressure measurements were being taken. Pressure profiles were taken with the probe

moving out (from high to low pressure) and with the probe moving in (from low to high pressure).

With the probe positioned to the extreme upstream position (the 1/4-in. tube pressed against the downstream face of the downstream probe support) the inert-gas side of the isolation valve was pressurized 2 or 3 inches of mercury above the predicted nozzle inlet pressure.

The isolation valve was opened, and the argon was injected into the probe and, consequently, the process system. After the null-pressure condition was reached, the probe drive mechanism was started and the probe was moved slowly outward. No additional argon was passed through the bubbler into the system; rather, as the probe moved out (from highest to lowest pressure), the argon in the pressure-probe assembly flowed out into the sodium stream. Here too, tests showed that continuous injection of not more than 8 cubic centimeters per minute of argon through the mineral-oil-filled bubbler into the system had no effect on the pressure measurements.

When the probe was moved inward (from low to high pressure), it was necessary to stop the probe, open the isolation valve, and permit the inert gas to depressurize by flowing into the sodium system. When the null-balance point was reached and the pressure measurement noted, the isolation valve was closed, and the argon lines up to the valve were repressurized in preparation for another axial pressure measurement.

General instrumentation and equipment. - As shown in figures 2 and 3 the U-shaped 10-foot length of 3-inch pipe, connecting the separator and the nozzle, is equipped with electrical heaters. Semicylindrical heaters placed on the straight sections of the pipe and tubular heaters located at the bends served as superheaters for the sodium vapor flowing from the separator. Power to these heaters was regulated manually with autotransformers.

Chromel-Alumel thermocouples were attached to the surface of the vapor line to facilitate control of the superheaters. Sheathed thermocouples were placed directly in the vapor stream upstream and downstream of the nozzle. Each isolation valve body was equipped with a thermocouple to ensure that the valve temperature was above the freezing temperature of sodium.

The wall static pressures were read on a mercury manometer. The acquisition of these data was entirely manual.

The axial-static-pressure probe was attached through the tie-rod connector to a pneumatic actuator (figs. 2 and 3). Instrument air was introduced to the actuator by a motorized pressure regulator. Fifteen minutes were required for a traverse with the probe. A rectilinear potentiometer attached to the connector was used to determine the position of the probe. The distance from the bellows housing to the tie-rod connector was determined frequently with a micrometer to check the potentiometer calibration. The millivolt output of the potentiometer was recorded on the Y-axis of a dual-axis recorder.

The axial pressure was read from a manometer; it was also sensed by an

unbonded strain-gage pressure transducer. The millivolt output of the transducer was recorded on the X-axis of the dual-axis recorder.

PROCEDURE

Operating Conditions

The nozzle research assembly was pretested with air at ambient temperature prior to installation in the sodium facility. The moisture content of the air was 1.5 grains per pound of air; this low moisture content precluded any significant effect on the expansion process due to condensation. The nozzle inlet pressure was varied from 10.45 to 29.67 inches of mercury absolute.

In the sodium facility, the nozzle inlet pressure was varied from 5.85 to 28.90 inches mercury absolute, while the receiving pressure was varied from 1.04 to 6.89 inches of mercury absolute. The vapors were heated to attain dry conditions before expansion. Up to 60° F superheat, as indicated by a rise in temperature between the separator and nozzle inlet locations 1 and 2 (fig. 2), was used.

Recording of Data

The wall-static-pressure data for both air and sodium flow were visually noted and manually recorded. The manometer readings were corrected to 32° F and recorded as inches of mercury absolute with a mercury column located on site to determine atmospheric pressure.

The wall-static-pressure data for air are tabulated in table I. Three different runs are tabulated at nozzle inlet pressures of 29.67, 20.10, and 10.45 inches of mercury absolute. Runs 1, 2, and 3 were made with low receiving pressures, which resulted in essentially no recompression. Only one set of observations is recorded in table I for each run; however, duplicate readings showed no deviations from the initial observations.

The wall-static-pressure data for sodium vapor are tabulated in table II. Runs 1 to 4 were made with the axial probe inserted, and runs 5 to 8 were made with the probe removed. After the process had operated at steady-state conditions for at least 1 hour as indicated by temperature at state points 1, 2, 4, and 5 (fig. 2), the initial set of wall-pressure readings was taken and recorded; the initial readings are designated as A. A set of repeated readings were taken immediately thereafter and designated as AA. In runs 1 to 5, after 1 to 6 hours of further operation at essentially the same process conditions, a second set of observations was made and partly or completely repeated. Table II shows the pressure readings corrected to a temperature of 32° F and the corresponding pressure ratios p_x/p_2. Where available, the measured value of the nozzle inlet pressure p_2 was used as the common denominator. In several instances, the inlet pressure tap was plugged, and the value of the inlet pressure was approximated by an extrapolation of the available pressure data to the nozzle inlet. These estimated values are designated in table II by foot-

note. It may be noted that where values of nozzle inlet pressure were measured, they were essentially the same as the pressure at wall-pressure tap 1. These estimated values are considered to be as correct as the reproducibility between repeated readings. Also listed are the temperature data taken during each set of pressure readings. Various degrees of superheat were used as shown in the third column of the temperature data.

The axial-probe static-pressure readings for air are not tabulated. Excellent reproducibility between the continuous pressure-length traces was obtained on the dual recorder with the probe traveling in either direction. An actuator drive speed to cover the nominal 3.8 inches of travel in 15 minutes was determined to be the fastest allowable speed. At faster probe speeds, the transmitted pressure to the transducer (and manometer) lagged behind the actual nozzle pressure. In order to determine this, the probe was stopped periodically, and the change of the pressure-recording pen on the dual-axis recorder and the corresponding change on the manometer were noted. The axial pressures for air in figures 6 and 7 are presented graphically only and are reproductions of the original traces.

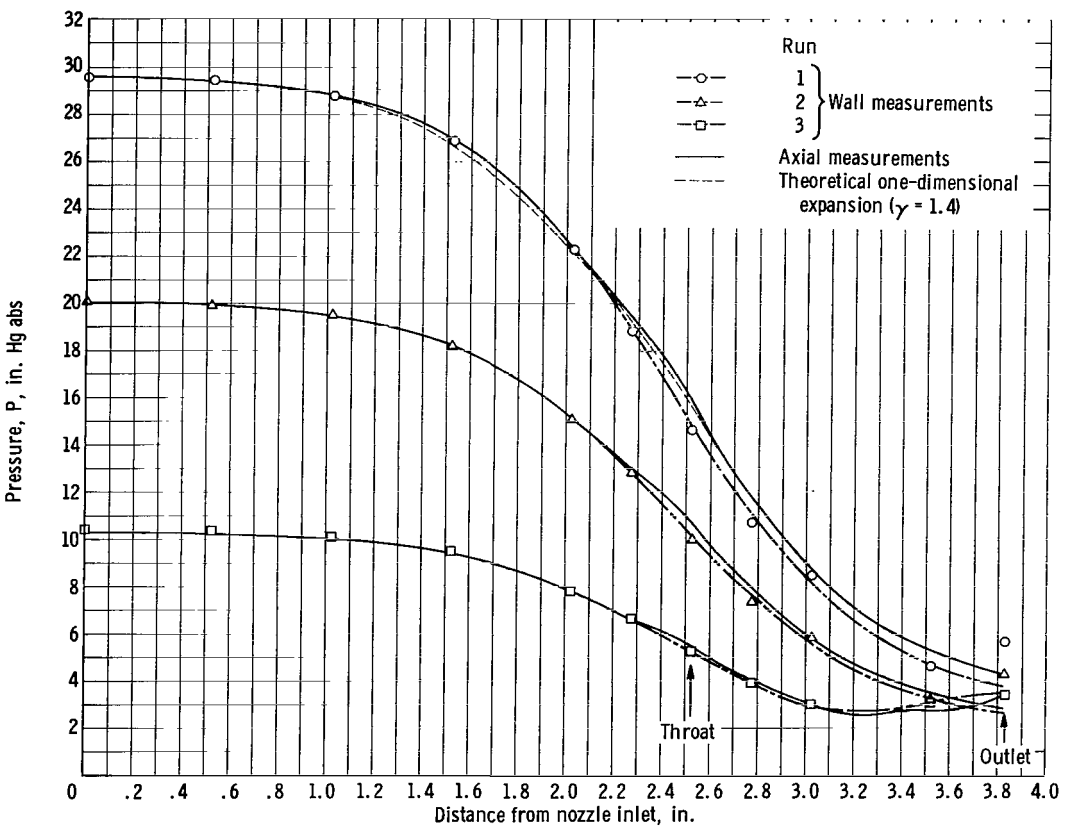

Figure 6. - Pressure distribution of air through nozzle. Inlet temperature, 55° F.

The axial-static-pressure data for sodium are tabulated in table III. An error as high as 0.3 inch of mercury between the pressure trace and the actual nozzle pressure at a particular location in the nozzle was noticed when the

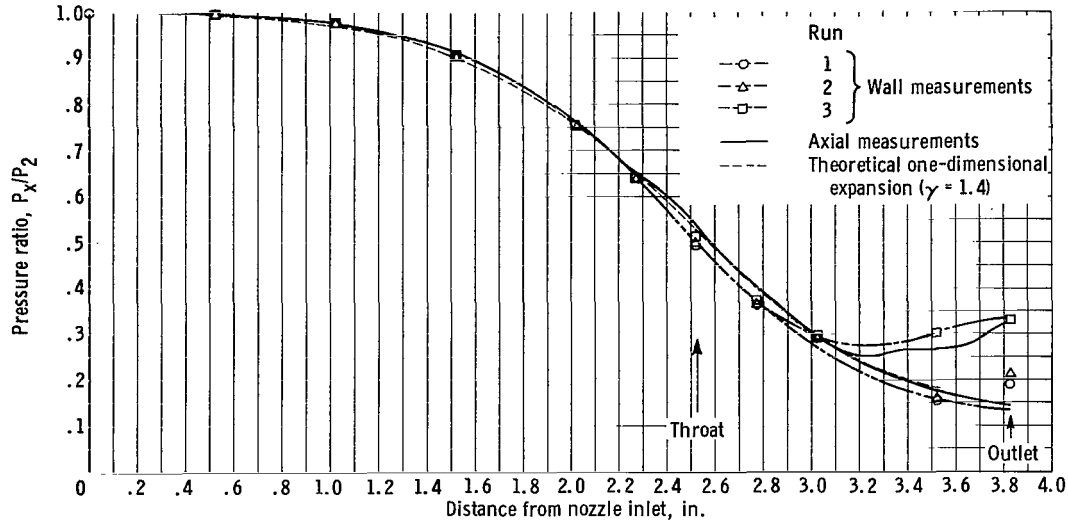

Figure 7. - Variation of static- to inlet-pressure ratio along nozzle wall and axis (air). Inlet temperature, 55° F.

probe was in motion. This value was determined by stopping the probe at various locations in the nozzle. At the inlet and the outlet of the nozzle, little error was noticed; however, as the pressure gradient increased, the error in transmitted reading increased up to about 0.3 inch of mercury. The lag in transmitted pressure was due to a larger volumetric transfer system than that used with the air-evaluating facility. Therefore, the probe was stopped at intervals, and the pressure output as measured by a manometer was recorded as shown in table III.

Table III contains data from four primary runs. These runs, designated 1 to 4, correspond to wall static data numbered similarly. Each run of axial-pressure data consists of two or more repeated tests that are lettered chronologically. The process temperature data are listed for each set of data and indicate stable operation throughout each primary run. The value of the nozzle inlet pressure p_2 was determined by a plot of the axial-pressure data and an extrapolation to the nozzle inlet. This extrapolated value did not differ significantly from the farthest upstream position of the probe pressure tap, which was about 1/8 inch downstream of the nozzle inlet.

Analysis of Data

The experimental data have been compared with the theoretical isentropic expansion of a gas as expressed by the following equation, where one-dimensional flow is assumed:

$$\frac{A_x}{A_t} = \frac{\left[\left(\frac{n-1}{n+1}\right)\left(\frac{2}{n+1}\right)^{2/(n-1)}\right]^{1/2}}{\left[\left(\frac{p_x}{p_2}\right)^{2/n} - \left(\frac{p_x}{p_2}\right)^{(n+1)/n}\right]^{1/2}}$$

A derivation of this equation is presented in appendix B as applicable to any substance undergoing a reversible process according to the relation $pv^n = c$. Since the equation also holds for a perfect gas, the substitution of γ for n allowed the use of the values tabulated in reference 5. In order to find the expansion process index, the sum of the squares of the differences between the observed values of p_x/p_2 and the theoretical pressure ratios for various values of n (or γ) were graphically minimized. This procedure is outlined in appendix C.

DISCUSSION OF RESULTS

Flow Characteristics of Air Through Experimental Nozzle

The pressure profiles for air flowing through the convergent-divergent nozzle are shown in figures 6 and 7. Figure 6 shows the variation of pressure through the nozzle for three different inlet pressures. Slight recompression at the outlet of the nozzle is noted for run 3. The theoretical isentropic expansion curve for air ($\gamma = 1.4$) is shown as a dotted line for run 1 for general comparison with experimental data. Up to 2.2 inches from the nozzle inlet, the wall- and axial-pressure measurements show excellent agreement and deviate only slightly from the theoretical curve. From 2.2 inches to the outlet of the nozzle, substantial difference between the wall and the axial measurements was observed. This is a departure from uniformity of flow as assumed in the one-dimensional analysis.

The wall measurements are lower than the axial pressures because of the curvature of the streamlines around the curved surface at the throat of the nozzle. Due to the resulting centrifugal forces, the pressure increases from the wall to the axis. The flow in this transonic region is supersonic near the wall at the geometric throat and is subsonic at the axis. Sonic speed is reached at the centerline downstream of the geometric throat of the nozzle. This nonuniformity persists to the nozzle outlet.

At about 2.2 inches from the nozzle inlet, the axial measurements show a decrease in the pressure gradient up to the throat where the gradient increases to a point 2.6 inches from the nozzle inlet. Beyond this point, the axial measurements again exhibit excellent conformity to the theoretical one-dimensional expansion. This temporary departure of the axial pressure from the theoretical in the transonic region may be due to a compression shock of unknown origin interacting with the boundary layer to exert pronounced changes in the flow

pattern (ref. 6).

The air data are shown in figure 7 as the variation of pressure ratio through the nozzle. The axial data coincide (up to the point of recompression in run 3) and indicate the plausibility of the one-dimensional analysis. The wall measurements also show good agreement and, as in figure 6, show departures from the axial data.

Flow Characteristics of Sodium Vapor Through Nozzle

Wall-pressure data. - The variation of pressure through the nozzle as measured by wall taps is shown in figure 8 for the eight runs made with nozzle inlet pressures ranging from 5.85 inches of mercury (run 6) to 28.90 inches of mercury (run 4). Some recompression is noted at the nozzle outlet for runs 1, 4, and 8. Theoretical expansion curves for various isentropic indexes are shown as dotted lines. Near the inlet of the nozzle, experimental data indicated generally a process index of 1.2 or less. Where the pressure gradient becomes fairly large at about 2.2 inches from the nozzle inlet, the data indicate (with the exception of run 4A) a process index of about 1.3. Run 4A was made with 33° F superheat and shows the anomaly of temporarily reduced pressure gradient in the transonic regime as noted previously with the axial-pressure data with air flow. A

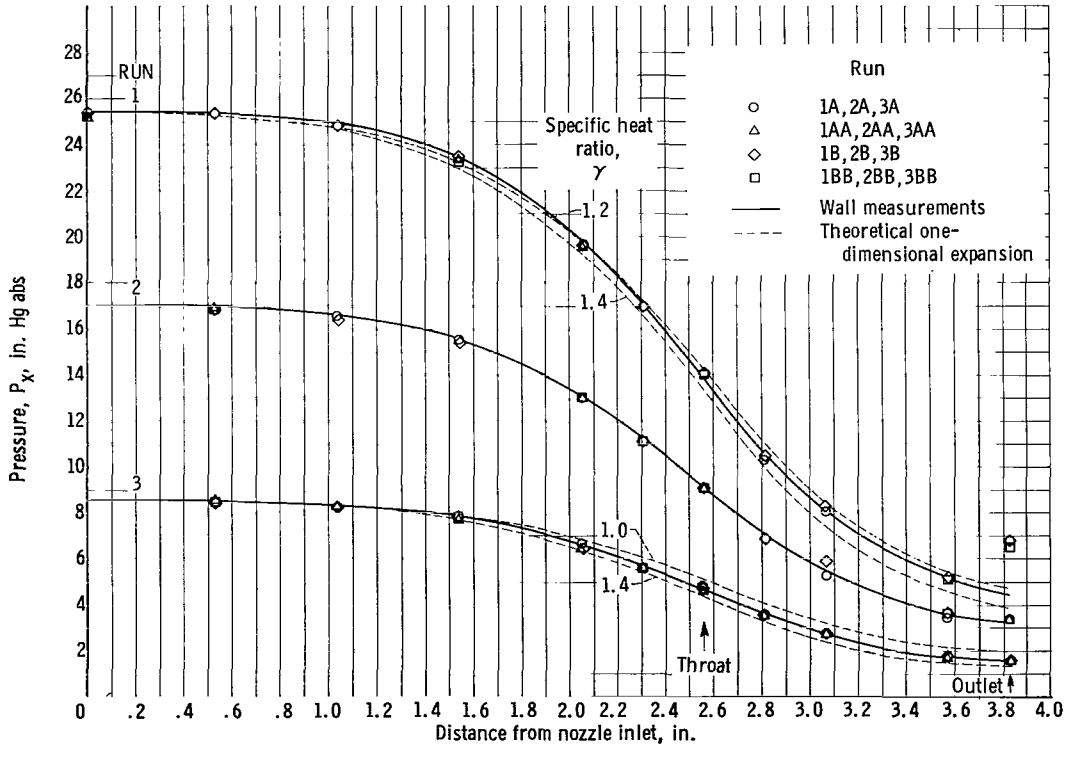

(a) Runs 1 to 3.

Figure 8. - Variation of wall pressure measurements through nozzle (sodium vapor).

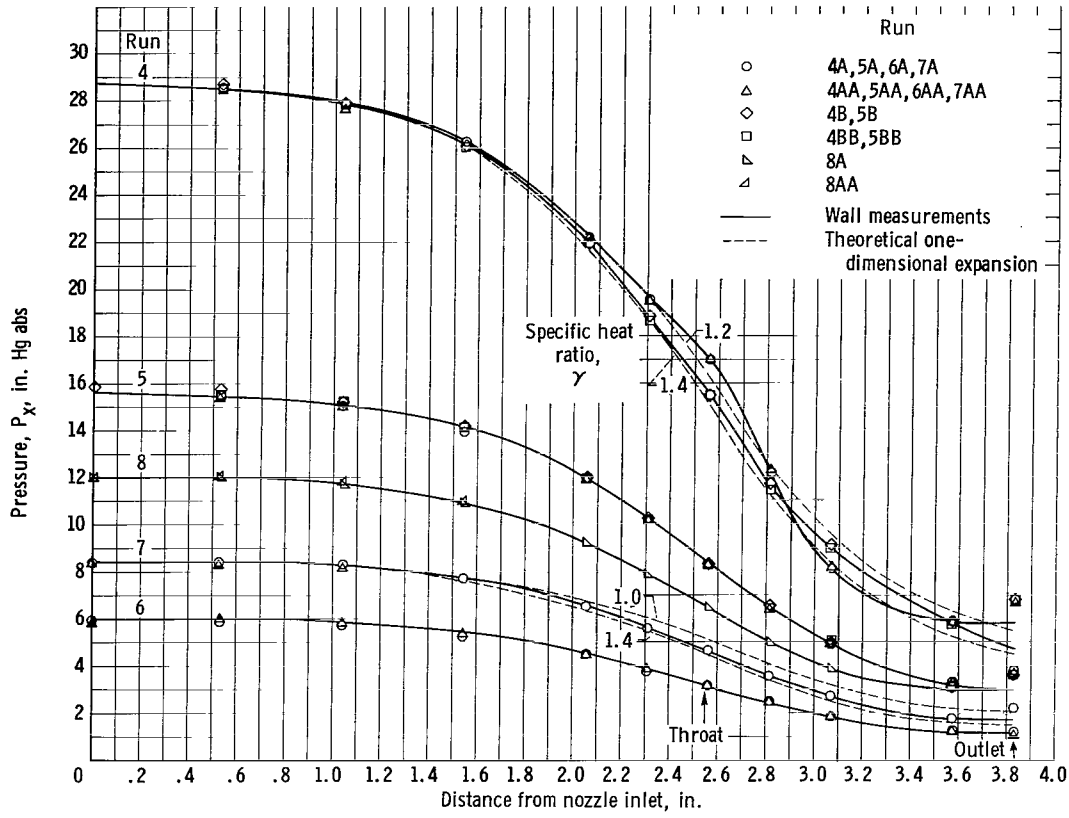

(b) Runs 4 to 8.

Figure 8. - Concluded. Variation of wall pressure measurements through nozzle (sodium vapor).

disturbance of the flow for this run is also noted in the supersonic region between nozzle taps 7 and 9. At tap 8, the process index appears to be 1.45.

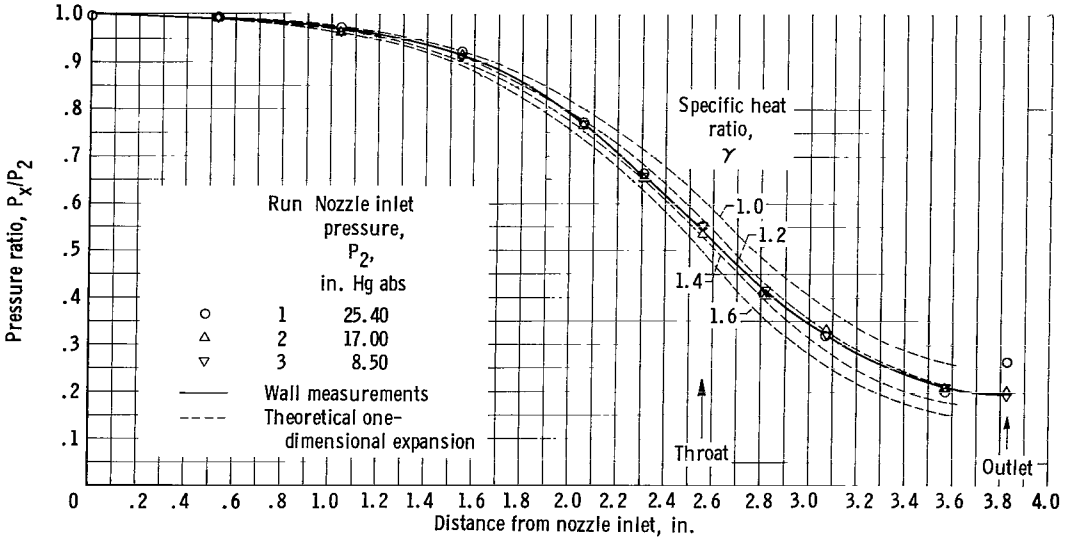

(a) Runs 1 to 3.

Figure 9. - Variation of static- to inlet-pressure ratio along nozzle wall (sodium vapor).

The data are shown as the variation of pressure ratio p_x/p_2 through the nozzle in figure 9. By inspection runs 1, 2, and 3 (fig. 9(a)) show an expansion index of about 1.3. In figure 9(b), run 4A indicates an expansion index as low as 1.05 at the throat. Run 4B shows an expansion index of 1.35 to 1.4. Runs 5 to 8 (fig. 9(c)) exhibit expansion indexes between 1.3 and 1.4 when neglecting the slight recompression at the nozzle outlet.

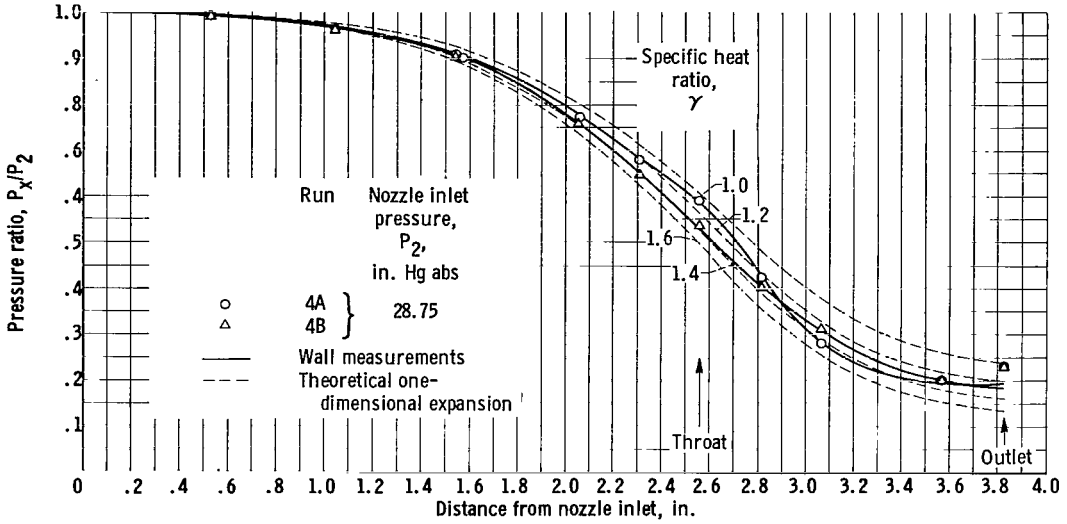

(b) Run 4.

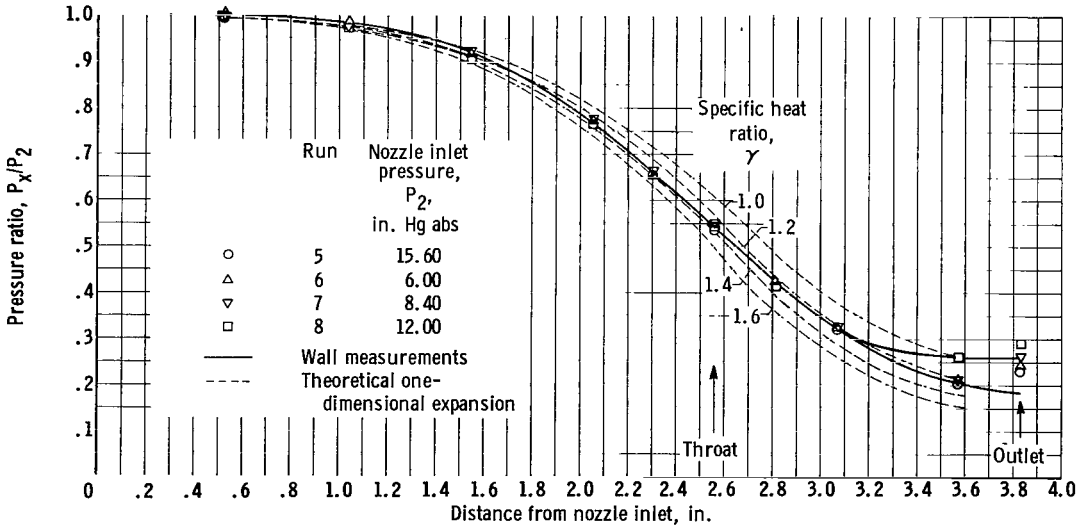

(c) Runs 5 to 8.

Figure 9. - Concluded. Variation of static- to inlet-pressure ratio along nozzle wall (sodium vapor).

The wall-pressure data for each run were treated as discussed in appendix C to determine the best approximation of the expansion process index for (1) the convergent section, (2) the divergent section, and (3) the overall expansion

process. Also the ratio of the pressure as measured at the throat of the nozzle to the nozzle inlet pressure p_t/p_2 was used to calculate the process index by means of equation (B10) of appendix B. These results together with the conditions at the nozzle inlet are summarized for each run in the following table:

Run	Nozzle inlet			Expansion process index, n			
	Pressure, p, in. Hg abs	Temperature, T, °F	Superheat, °F	At throat, n_t	Convergent section, n_c	Divergent section, n_d	Overall, n_o
1	25.40	1613	20	1.26	1.26	1.26	1.26
2	17.01	1526	10	1.35	1.35	1.28	1.29
3	8.58	1443	35	1.25	1.29	1.23	1.25
4A	[a]28.70	1647	33	1.06	1.16	1.24	1.24
4B	[a]28.83	1624	9	1.34	1.38	1.29	1.32
5A	[a]15.42	1504	0	1.33	1.29	1.27	1.27
5B	[a]15.74	1565	62	1.40	1.42	1.32	1.33
6	5.90	1383	35	1.30	1.27	1.27	1.32
7	8.41	1423	23	1.28	1.27	1.23	1.22
8	12.08	1482	23	1.33	1.33	1.27	1.30

[a]Extrapolated values.

The only significant difference between these expansion indexes, as calculated by the method of appendix C, is for the convergent section of the nozzle for runs 4A and 5B. Run 4A was made with 33° F superheat and shows a convergent expansion index n_c of 1.16. Run 5B with 62° F superheat shows a value of 1.42 for the index. Comparison of runs 1, 7, and 8, with runs 3, 4A, and 6, which were made with essentially the same superheat, indicate no effect of nozzle inlet pressure (or temperature) on the index. Similarly, no effect on the value of the index is noted with varied levels of superheat notwithstanding the differences in the index between runs 4A and 5B. It is noted that the expansion process index n_t as determined by the static pressure measured at the throat of the nozzle, with the exception of run 4A, is not significantly different from the other indexes determined by use of all the available data. Runs 5 to 8, which were made with the axial probe removed, are not significantly different from runs 1 to 4, which were made with the probe inserted.

Since no significant trends in the process index are apparent, all the data are consolidated to determine values of the convergent, the divergent, and the overall expansion indexes (n_c, n_d, and n_o), as outlined in appendix C.

Also an average value of throat expansion index n_t obtained from the average value of p_t/p_2 for the runs was determined. These values are given in the following table:

Expansion process index, n	Numerical value
At throat, n_t	1.29
Convergent section, n_c	1.32
Divergent section, n_d	1.27
Overall, n_o	1.28

Axial-pressure data. - The pressure distributions through the nozzle as determined by the axial probe are shown in figure 10. The four runs were made with essentially the same operating conditions as those for the corresponding wall-pressure readings, with the exception of run 4A, which was made with 33° F superheat when the wall data were being recorded and 10° F superheat when the search probe data was being obtained. This is noted by a comparison of tables II and III in which the wall-tap data and the axial-pressure data, respectively,

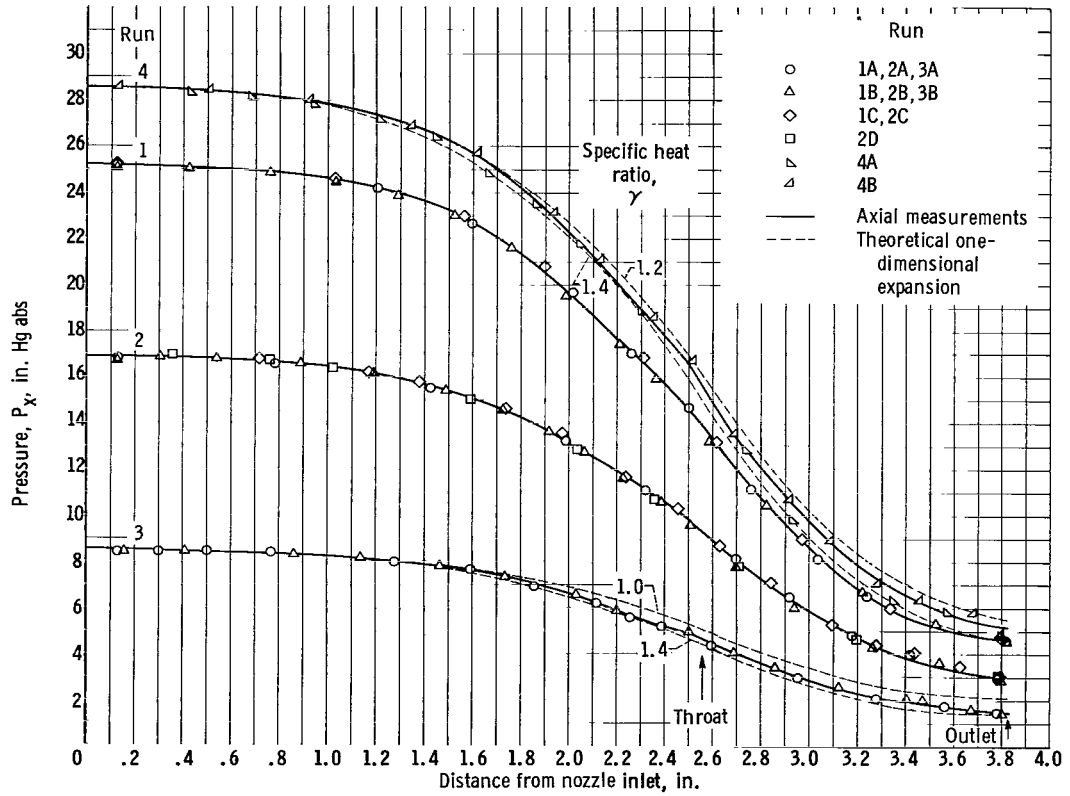

Figure 10. - Variation of axial pressure measurements through nozzle (sodium vapor).

are given. Generally, after the desired process conditions were established, a set of wall-tap pressure measurements were taken, followed by the axial measurements; a second set of wall-tap measurements were taken before the process conditions were changed. For each run in tables II and III the process conditions are listed for reference.

The axial search tube was used primarily to attempt to locate the zone of condensation of the vaporous sodium as well as to obtain general pressure profiles through the nozzle. No changes in the pressure gradient that would be indicative of condensation were noted.

Figure 10 shows an expansion index of about 1.3 when the recompression at the outlet of the nozzle is neglected. A slight indication of the temporary decrease in the pressure gradient just ahead of the throat of the nozzle is noted as also observed with the air data.

All the axial-pressure data are plotted in figure 11 as the variation of pressure ratio through the nozzle. No effect of pressure level or superheat is indicated. The curve drawn through the data neglects the anomalous points just upstream of the throat and those indicating slight recompression at the nozzle outlet.

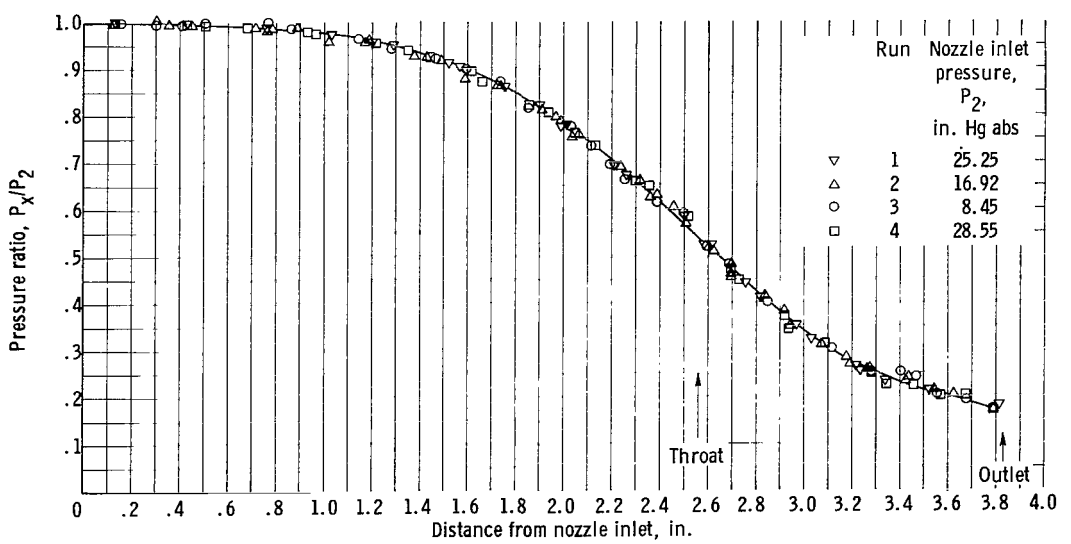

Figure 11. - Variation of static- to inlet-pressure ratio along nozzle axis (sodium vapor).

All the data for the flow of sodium vapor through the nozzle are summarized in figure 12. The curve drawn through the axial-pressure data (fig. 11) is shown as a solid curve in figure 12. At each wall tap, the average pressure ratio for all runs is shown together with the high and low values of the pressure ratio. Theoretical-expansion curves for various isentropic indexes are shown as dotted lines. With the exception of the wall-tap readings at taps 8 and 9, which reflect some recompression, the axial-pressure curve passes through the mean value of each wall-tap measurement. Inspection of figure 12 reveals that the expansion process index indicated by both wall- and axial-pressure

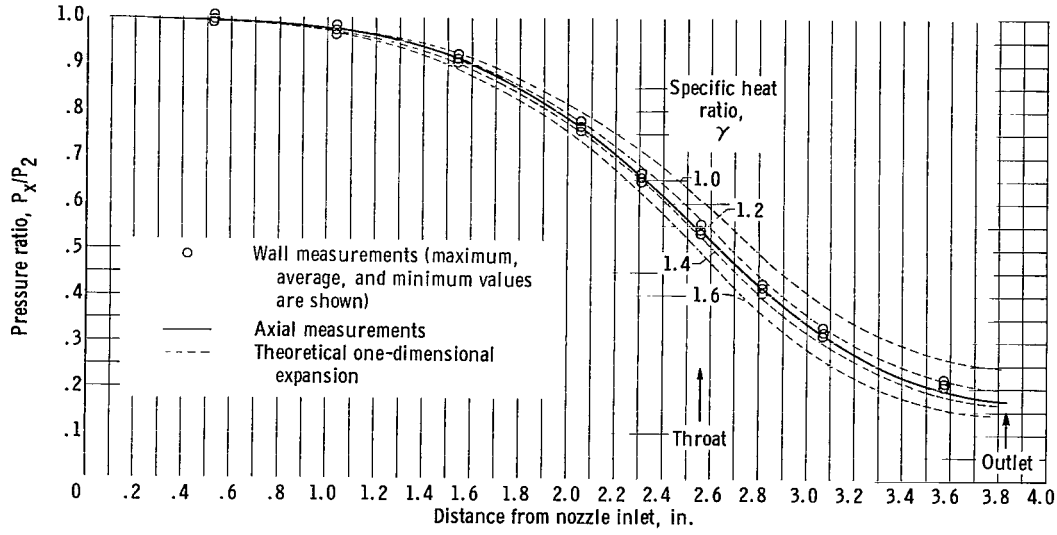

Figure 12. - Variation of static- to inlet-pressure ratio along nozzle wall and axis.

data is about 1.3.

The condition of the vapors entering the nozzle was defined entirely on the basis of pressure and temperature measurements. Without an additional means of ascertaining the quality of the vapor, the possibility exists that true superheat may not have been attained; that is, liquid droplets could have been dispersed in the superheated vapor. The presence of droplets could have affected the expansion process and the resulting index. Consequently, further study at higher levels of superheat together with accurate measurements of flow are needed. The expansion index, as determined herein, also includes the effect of friction in the nozzle; for example, if the nozzle efficiency were 95 percent, the isentropic index would be about 1.33. More accurate determination of the isentropic index would, therefore, require knowledge of the actual efficiency of the nozzle.

Thermal growth corrections. - The accuracy of the position at which the probe static pressures were measured depended on the thermal growth of the pressure tap from the downstream strut, which served as a reference stop. For thermal growth corrections, it was assumed that the entire probe was at the receiving temperature (state 4). The static temperature difference between the nozzle inlet (state 2) and the receiving zone (state 4) was not greater than 300° F. If the entire probe were at the inlet temperature, the maximum error in the approximate 4 inches of travel would be 0.15 inch and would occur when the probe tap was located at the nozzle inlet. At the nozzle outlet, there would be essentially no error. Over the complete traverse, therefore, the errors involved in assuming the entire probe to be at the receiving temperature are considered to be insignificant or well within the accuracy of plotting the data as seen by inspection of figures 11 and 12. In the region of the tie-rod connector, to which the rectilinear potentiometer was connected, the temperature was about 300° F and was maintained by electrical heaters. Consequently, it was also assumed that no significant errors in position were introduced from

this source.

The temperatures used for the thermal growth of the nozzle were measured by a surface-welded thermocouple located at the middle of the 4-inch-long nozzle. The error involved in the corrected position of a wall tap is not greater than ±0.005 inch.

Vapor-pressure check. - As a check on the pressure-measuring technique, the nozzle inlet and the receiving pressures were compared with a vapor-pressure curve recommended in reference 4. The result is shown in figure 13.

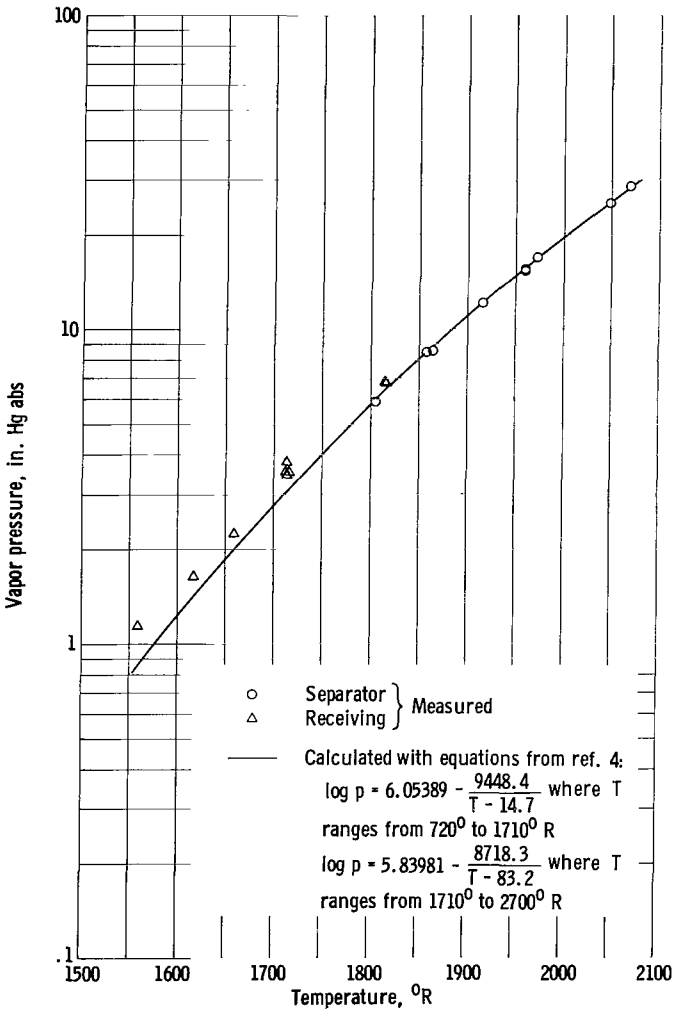

Figure 13. - Comparison of measured pressures with pressures calculated with equations from reference 4.

The pressure measured at the nozzle inlet (state 2) should (with line losses neglected) be the same as the saturation pressure in the separator. Likewise, the measured pressures at the tee downstream of the nozzle should correspond with the saturation pressure in the condenser (state 5). In figure 13, the pressure measured at the nozzle inlet is plotted against the temperature measured in the separator. The measured pressures range from 5.97 to 28.58 inches of mercury and show excellent agreement with the vapor-pressure curve.

The measured receiving pressures, also indicated in figure 13, fall above the recommended vapor-pressure curve. These measured pressures are plotted against the temperature of the saturated condensate measured in the bottom header of the free-draining condenser (state 5). If it is assumed that the recommended vapor-pressure curve is accurate in the low pressure area, the partial pressure of the inert gas, injected for pressure measurement, in the area of the condenser and the pressure losses from the tee to the bottom of the condenser probably account for the discrepancies.

SUMMARY OF RESULTS

An inert-gas-injection technique has been successfully used to measure accurately the pressure of vaporous sodium flowing under steady-state conditions through an axisymmetrical convergent-divergent nozzle. Nozzle inlet conditions were varied; pressures ranged from approximately 6 to 29 inches of mercury absolute, while inlet temperatures ranged from 1380° to 1650° F with indicated superheat up to 60° F above saturated temperature. Pressure distributions through the nozzle were determined with wall taps and an axial-pressure probe and were compared with the pressure distributions theoretically calculated for a gas expanding isentropically. The following results were found:

1. The accuracy of pressure measurements of one- or two-phase flow obtainable by the inert-gas-injection technique depends upon the sensitivity of the read-out instrument. This technique is recommended for use in high-temperature liquid-phase and vapor-phase liquid-metal systems, where proper analysis of research data requires the measurement of process pressures to an accuracy of a few inches of water.

2. The axial pressure distribution along the nozzle axis did not differ significantly from the distribution determined by the wall pressure taps. No changes in the pressure gradient that would be indicative of condensation were noted. Also, no significant difference in the expansion path as a function of superheat for indicated superheats up to 60° F was noted.

3. A value of 1.3 for the expansion index relating the pressure and volume during expansion according to $pv^n = c$ best represented the nozzle and the test conditions investigated. Further study at higher levels of superheat together with accurate measurements of flow are needed to substantiate the results. True superheat may not have been attained; that is, liquid droplets could have been dispersed in the superheated vapor.

Lewis Research Center
National Aeronautics and Space Administration
Cleveland, Ohio, January 22, 1964

APPENDIX A

SYMBOLS

A	area, sq ft
c	constant
g	conversion constant, 32.17 (lb-mass/lb-force)(ft/sec^2)
J	mechanical equivalent of heat, 778.2 ft-lb/Btu
n	process expansion index
p	absolute pressure, lb/sq in., or in. Hg abs
r	ratio of pressure at any location to inlet pressure
T	temperature, ^{o}F
u	internal energy, Btu/lb
V	velocity, ft/sec
v	specific volume, cu ft/lb
W	work, Btu/lb
w	weight flow, lb/sec
γ	ratio of specific heat at constant pressure to specific heat at constant volume
1	separator vapor outlet
2	nozzle inlet
3	nozzle outlet
4	condenser inlet
5	condenser outlet

Subscripts:

c	convergent section of nozzle
d	divergent section of nozzle
o	overall (convergent and divergent sections of nozzle)
obs	observed or measured

t throat of nozzle

x variable state point

γ theoretical

APPENDIX B

DERIVATION OF EQUATION RELATING PRESSURES AND AREA IN ONE-DIMENSIONAL ISENTROPIC NOZZLE EXPANSION

In one-dimensional analysis of steady-state flow, it is assumed that the radius of curvature of the ducting is much larger than the width of the ducting and that the properties of the flowing fluid change only in the axial direction. This implies that any properties required to define the flowing fluid are constant at any plane normal to the stream and that transverse flow does not exist. This is, of course, not true. By working with average transverse values of the defining properties, however, this one-dimensional analysis gives a good indication of the average change in properties along the longitudinal coordinate.

In many cases, flow through a short well-contoured nozzle is essentially frictionless, and the expansion process can be considered reversible. Small deviations from a frictionless expansion can best be expressed by a nozzle efficiency factor or a velocity coefficient. The expansion process through a short nozzle is essentially adiabatic because of the small heat-transfer area available and the short residence time of the flowing fluid in the nozzle. This reversible adiabatic (or isentropic) expansion is a valuable guide for comparing actual expansion processes.

The following derivation relates the area at any location in a convergent-divergent nozzle to the pressure at the same location, the inlet pressure, and the area of the throat of the nozzle for critical flow. One-dimensional isentropic flow is assumed in the derivation.

The general energy equation for isentropic flow in the nozzle from the inlet to any station within the nozzle can be written as

$$u_2 - u_x = \frac{1}{J}\left[\frac{V_x^2}{2g} - \frac{V_2^2}{2g} + p_x v_x - p_2 v_2\right] \tag{B1}$$

The change in internal energy is independent of the process occurring between state points whether that process is flow or nonflow. Therefore, the simple energy equation for an isentropic nonflow process can be utilized to show that

$$u_2 - u_x = W = \frac{1}{J}\int_2^x p\, dv \tag{B2}$$

From equations (B1) and (B2),

$$\int_2^x p\,dv = \frac{1}{2g}\left[V_x^2 - V_2^2\right] + p_x v_x - p_2 v_2 \tag{B3}$$

If it is assumed that the expansion occurs according to the formula $pv^n = c$, equation (B3) becomes

$$c\int_{v_2}^{v_x} \frac{dv}{v^n} = \frac{1}{2g}\left[V_x^2 - V_2^2\right] + p_x v_x - p_2 v_2 \tag{B4}$$

Integrating the left term of equation (B4) and rearranging by means of the relation $p_2 v_2^n = p_x v_x^n = c$ reduce equation (B4) to

$$\frac{cv_x^{1-n} - cv_2^{1-n}}{1 - n} = \frac{p_x v_x - p_2 v_2}{1 - n} = \frac{1}{2g}\left[V_x^2 - V_2^2\right] + p_x v_x - p_2 v_2 \tag{B5}$$

which holds for any substance undergoing a reversible process according to the relation $pv^n = c$.

From equation (B5) the velocity at state x is expressed in the following equation:

$$V_x = \left\{\frac{2gnp_2v_2}{1 - n}\left[\left(\frac{p_x}{p_2}\right)^{(n-1)/n} - 1\right]\right\}^{1/2} \tag{B6}$$

where the initial velocity V_2 is assumed to be negligible. The weight flow through the nozzle can be found from the continuity equation

$$w = \frac{A_x V_x}{v_x} \tag{B7}$$

and equation (B6) by means of $v_x = v_2(p_2/p_x)^{1/n}$,

$$w = A_x\left\{\frac{2gnp_2}{v_2(n - 1)}\left[\left(\frac{p_x}{p_2}\right)^{2/n} - \left(\frac{p_x}{p_2}\right)^{(n+1)/n}\right]\right\}^{1/2} \tag{B8}$$

Equation (B8) is applicable for any pressure p_x when the process expansion

index n is known. For a perfect gas, the process index is γ, the ratio of the specific heat at constant pressure to the specific heat at constant volume c_p/c_v, where $pv^\gamma = c$ describes the expansion process. Writing equation (B8) for the throat of the nozzle and dividing this explicit form of the weight-flow equation by equation (B8) as shown previously give

$$\frac{A_x}{A_t} = \left[\frac{\left(\frac{p_t}{p_2}\right)^{2/n} - \left(\frac{p_t}{p_2}\right)^{(n+1)/n}}{\left(\frac{p_x}{p_2}\right)^{2/n} - \left(\frac{p_x}{p_2}\right)^{(n+1)/n}} \right]^{1/2} . \tag{B9}$$

The pressure ratio p_t/p_2 for critical flow is related to the process index as follows:

$$\frac{p_t}{p_2} = \left(\frac{2}{n+1}\right)^{n/(n-1)} \tag{B10}$$

Substitution of this equation into equation (B9) results in

$$\frac{A_x}{A_t} = \frac{\left[\left(\frac{n-1}{n+1}\right)\left(\frac{2}{n+1}\right)^{2/(n-1)}\right]^{1/2}}{\left[\left(\frac{p_x}{p_2}\right)^{2/n} - \left(\frac{p_x}{p_2}\right)^{(n+1)/n}\right]^{1/2}} \tag{B11}$$

This expression relates the ratio of the area at any location to the throat area, and the ratio of the pressure at station x to the inlet pressure for a reversible expansion.

APPENDIX C

DETERMINATION OF ISENTROPIC PROCESS INDEX

The best estimate of the process index n was determined for the wall static-pressure data by application of the principle of least squares. A process index was determined from (1) the nozzle inlet to and including the throat of the nozzle, (2) the throat of the nozzle to the outlet, and (3) the inlet to the outlet of the nozzle. This procedure was followed for each run as well as in the consolidation of all wall static-pressure readings.

The index was determined by calculation of the sum of the squares of the differences between the observed values of p_x/p_2 at the various tap locations and the theoretical pressure ratio determined by a specific value of n (or γ) (these values are given in ref. 5). This summation of the squares of the differences is noted by

$$\sum_{\text{tap 1}}^{9} (r_{obs} - r_{\gamma})^2 \qquad \gamma = \gamma_1, \gamma_2, \cdots \gamma_m \tag{C1}$$

where r_{obs} is the observed or measured pressure ratio p_x/p_2 at a specific pressure tap and r_{γ} is the theoretical pressure ratio corresponding to the area ratio at the particular pressure tap. The function

$$f(\gamma_i) = \sum_{\text{tap 1}}^{9} (r_{obs} - r_{\gamma,i})^2 \qquad \gamma_i = \gamma_1, \gamma_2, \cdots \gamma_m \tag{C2}$$

was minimized graphically by a plot of $f(\gamma)$ as a function of γ. The process index n, corresponding to the minimum value of the function, is tabulated in the section, DISCUSSION OF RESULTS.

REFERENCES

1. Coultas, T. A.: Thermodynamic Aspects of the Flow of Sodium Vapor Through a Supersonic Nozzle. Research Rept. 61-32, Rocketdyne Div., North American Aviation, Inc., Nov. 1961.

2. Nichols, Landon R., Winzig, Charles H., Nosek, Stanley M., and Goldman, Louis J.: Design and Operational Performance of a 150-Kilowatt Sodium Flash-Vaporization Facility. NASA TN D-1661, 1963.

3. Weatherford, W. D., Jr., Tyler, John C., and Ku, P. M.: Properties of Inorganic Energy-Conversion and Heat-Transfer Fluids for Space Applications. WADD TR 61-96, Nov. 1961.

4. Thomson, George W., Garelis, Edward: Physical and Thermodynamic Properties of Sodium. Second ed., Ethyl Corp., Nov. 29, 1955.

5. Keenan, Joseph H., Kaye, Joseph: Gas Tables. John Wiley & Sons, Inc., 1948. Tables 30-34.

6. Shapiro, Ascher H.: The Dynamics and Thermodynamics of Compressible Fluid Flow. Vol. 2, Ronald Press, 1954.

TABLE I. - NOZZLE WALL STATIC-PRESSURE DATA (AIR)

[Nozzle inlet temperature, 55° F.]

Wall tap location	Run					
	1		2		3	
	Pressure, p, in. Hg abs	Pressure ratio, p_x/p_2	Pressure, p, in. Hg abs	Pressure ratio, p_x/p_2	Pressure, p, in. Hg abs	Pressure ratio, p_x/p_2
Inlet	29.67	1.000	20.10	1.000	10.45	1.000
1	29.48	.993	19.94	.992	10.39	.994
2	28.79	.970	19.50	.970	10.15	.971
3	26.83	.904	18.17	.904	9.48	.907
4	22.25	.750	15.07	.750	7.83	.749
5	18.87	.636	12.80	.637	6.68	.639
6	14.64	.493	10.00	.498	5.33	.510
7	10.75	.362	7.38	.367	3.93	.376
8	8.55	.288	5.83	.290	3.09	.296
9	4.67	.157	3.25	.162	3.17	.303
Receiving	5.82	.196	4.38	.218	3.51	.336
Barometer	29.64	-----	29.49	-----	29.49	-----

TABLE II. - NOZZLE WALL STATIC-PRESSURE DATA (SODIUM VAPOR)

(a) Axial probe inserted

Run	Nozzle inlet (state 2)	Nozzle wall pressure tap									Condenser (states 4 and 5)	Barometer	Separator (state 1)	Nozzle inlet (state 2)	Degrees of superheat (state 2)	Nozzle discharge	Condenser inlet (state 4)	Condenser outlet (state 5)
		1	2	3	4	5	6	7	8	9								
	Pressure, p, in. Hg abs												Temperature, T, ^{o}F					
1A	25.49	25.38	24.84	23.49	19.77	16.97	14.09	10.39	8.10	5.12	6.89	29.33	1590	1611	21	1373	1357	1358
1AA	25.39	-----	-----	23.38	19.66	-----	-----	-----	----	----	----	↓		1611	21	1366	1358	1355
1B	25.45	25.40	24.87	23.50	19.67	16.97	14.04	10.54	8.37	5.28	6.87			1609	19	1365	1360	1355
1BB	25.28	-----	-----	23.28	-----	-----	14.02	-----	----	5.26	6.57			1608	18	1360	1356	1357
	Pressure ratio, p_x/p_2																	
1A	1.00	0.996	0.975	0.922	0.776	0.666	0.553	0.408	0.318	0.201	0.270							
1AA	↓	-----	-----	.921	.774	-----	-----	-----	-----	-----	-----							
1B		.998	.977	.923	.773	.667	.552	.414	.329	.208	.270							
1BB		-----	-----	.921	-----	-----	.555	-----	-----	.208	.260							
	Pressure, p, in. Hg abs																	
2A	[a]17.05	16.90	16.40	15.55	13.05	11.14	9.07	6.94	5.37	3.57	3.44	29.29	1513	1522	9	1270	1260	1256
2AA	------	16.93	-----	-----	12.97	-----	9.07	----	----	3.59	3.46	↓		1522	9	1270	1259	1257
2B	[a]16.97	16.78	16.40	15.46	13.17	11.15	9.16	6.89	5.97	3.77	3.49			1523	10	1270	1259	1256
2BB	------	16.90	-----	-----	13.02	-----	9.16	----	----	3.69	----			1523	10	1271	1260	1256
	Pressure ratio, p_x/p_2																	
2A	1.00	0.991	0.962	0.912	0.765	0.653	0.532	0.407	0.315	0.209	0.202							
2AA	↓	.993	-----	-----	.761	-----	.532	-----	-----	.211	.203							
2B		.989	.966	.911	.776	.657	.540	.406	.352	.222	.206							
2BB		.996	-----	-----	.767	-----	.540	-----	-----	.217	-----							
	Pressure, p, in. Hg abs																	
3A	[a]8.52	8.49	8.30	7.86	6.69	5.76	4.80	3.64	2.81	1.85	1.66	29.19	1405	1437	32	1198	1164	1158
3AA	[a]8.61	8.54	8.28	7.71	6.55	5.68	4.68	3.55	2.80	1.78	1.65	↓	1404	1439	35	1198	1165	1158
3B	[a]8.60	8.40	8.31	7.91	6.56	5.61	4.80	3.63	2.84	1.81	1.63		1405	1442	37	1196	1164	1161
3BB	-----	8.54	----	7.90	----	5.63	----	----	----	----	----		1405	1441	36	1190	1168	1161
	Pressure ratio, p_x/p_2																	
3A	1.00	0.997	0.974	0.923	0.785	0.676	0.563	0.427	0.330	0.217	0.195							
3AA	↓	.992	.962	.896	.761	.660	.544	.410	.325	.207	.192							
3B		.977	.966	.920	.763	.652	.558	.422	.330	.211	.190							
3BB		.993	-----	.919	-----	.655	-----	-----	-----	-----	-----							
	Pressure, p, in Hg abs																	
4A	[a]28.78	28.59	27.87	26.23	22.26	19.56	17.00	12.21	8.08	5.86	6.78	29.22	1610	1639	29	1365	1357	1356
4AA	[a]28.61	28.39	27.62	26.17	22.17	19.48	17.00	12.28	8.17	5.88	6.59	↓	1611	1648	37	1380	1358	1356
4B	[a]28.90	28.68	27.89	26.04	21.89	18.79	15.52	11.74	9.14	5.88	6.83		1612	1621	9	1366	1357	1355
4BB	[a]28.76	28.54	27.85	26.04	21.92	18.64	15.52	11.43	8.96	5.83	6.80		1612	1621	9	1365	1356	1355
	Pressure ratio, p_x/p_2																	
4A	1.00	0.993	0.968	0.911	0.774	0.680	0.591	0.424	0.281	0.204	0.236							
4AA	↓	992	.965	.915	.775	.681	.594	.429	.286	.206	.230							
4B		.992	.965	.901	.757	.650	.537	.406	.317	.204	.236							
4BB		.992	.968	.904	.762	.648	.540	.397	.312	.203	.236							

[a]Extrapolated data.

(b) Axial probe removed

Run	Nozzle inlet (state 2)	Nozzle wall pressure tap 1	2	3	4	5	6	7	8	9	Condenser (states 4 and 5)	Barometer	Separator (state 1)	Nozzle inlet (state 2)	Degrees of superheat (state 2)	Nozzle discharge	Condenser inlet (state 4)	Condenser outlet (state 5)
	Pressure, p, in. Hg abs												Temperature, T, °F					
5A	[a]15.42	15.44	15.07	14.01	11.96	10.19	8.38	6.57	4.96	3.31	3.83	29.38	1500	1500	0	1270	1261	1258
5AA	[a]15.42	15.35	15.02	14.08	11.99	10.12	8.31	6.41	4.98	3.31	3.75	↓	1501	1501	0	1267	1259	1257
5B	15.84	15.68	15.15	14.18	11.97	10.32	8.38	6.40	5.02	3.05	3.50		1500	1562	62	1263	1254	1251
5BB	[a]15.64	15.57	15.23	14.12	11.94	10.15	8.22	6.40	4.99	3.09	3.56		1500	1561	61	1277	1253	1254
	Pressure ratio, p_x/p_2																	
5A	1.00	1.00	0.977	0.909	0.776	0.661	0.543	0.426	0.322	0.215	0.248	29.38						
5AA	↓	.996	.974	.913	.778	.656	.539	.416	.323	.215	.243	↓						
5B		.990	.956	.895	.756	.652	.529	.404	.317	.193	.221							
5BB		.996	.974	.903	.763	.649	.526	.409	.319	.198	.228							
	Pressure, p, in. Hg abs																	
6A	5.96	5.89	5.74	5.32	4.56	3.81	3.21	2.51	1.91	1.29	1.27	29.14	1344	1379	35	1117	1106	1098
6AA	5.85	6.02	5.93	5.46	4.57	3.89	3.23	2.51	1.92	1.26	1.04	29.14	1346	1381	35	1121	1113	1105
	Pressure ratio, p_x/p_2																	
6A	1.00	0.988	0.963	0.893	0.765	0.639	0.539	0.421	0.321	0.216	0.213	29.14						
6AA	1.00	1.029	1.014	.933	.781	.665	.552	.429	.328	.215	.178	29.14						
	Pressure, p, in. Hg abs																	
7A	8.42	8.45	8.31	7.76	6.56	5.59	4.63	3.61	2.77	1.80	2.24	29.14	1400	1422	22	1208	1201	1200
7AA	8.40	8.36	8.14	----	----	----	----	----	----	----	----	29.14	1395	1418	23	1207	1200	1198
	Pressure ratio, p_x/p_2																	
7A	1.00	1.004	0.987	0.922	0.779	0.664	0.550	0.429	0.329	0.214	0.266	29.14						
7AA	1.00	.995	.969	-----	-----	-----	-----	-----	-----	-----	-----	29.14						
	Pressure, p, in. Hg abs																	
8A	12.05	12.02	11.66	10.88	9.22	7.88	6.52	4.98	3.91	3.14	3.52	29.16	1456	1479	23	1265	1258	1260
8AA	12.10	12.07	11.78	10.99	----	----	----	----	----	----	----	29.16	1457	1479	22	1265	1257	1259
	Pressure ratio, p_x/p_2																	
8A	1.00	0.998	0.968	0.903	0.765	0.654	0.541	0.413	0.325	0.261	0.292							
8AA	1.00	.998	.974	.908	-----	-----	-----	-----	-----	-----	-----							

[a]Extrapolated data.

TABLE III. - AXIAL PRESSURE DATA (SODIUM VAPOR)

Run 1A			Run 1B			Run 1C		
Probe pressure tap position from nozzle inlet, in.	Pressure, p, in. Hg abs	Pressure ratio, p_x/p_2	Probe pressure tap position from nozzle inlet, in.	Pressure, p, in. Hg abs	Pressure ratio, p_x/p_2	Probe pressure tap position from nozzle inlet, in.	Pressure, p, in. Hg abs	Pressure ratio, p_x/p_2
Probe travel: outward			Probe travel: inward			Probe travel: outward		
0.126	25.23	0.999	0.126	25.08	0.999	0.126	25.30	0.999
1.206	24.21	.959	.423	25.05	.998	1.031	24.61	.972
1.599	22.71	.899	.760	24.84	.990	1.566	23.00	.908
2.013	19.72	.781	1.033	24.51	.977	1.901	20.81	.822
2.267	17.11	.678	1.291	23.88	.951	2.308	16.86	.666
2.500	14.72	.583	1.524	22.98	.916	2.618	13.22	.522
2.758	11.18	.443	1.758	21.64	.862	2.972	8.99	.355
3.037	8.15	.323	1.990	19.54	.778	3.335	6.02	.238
3.237	6.52	.258	2.210	17.47	.696	3.807	4.69	.185
3.818	4.62	.183	2.367	15.94	.635	Condenser	6.87	0.271
Condenser	6.89	0.273	2.587	13.22	.527	Barometer	29.32	-----
Barometer	29.32	-----	2.819	10.44	.416			
			3.219	6.70	.267	Location	State	Temperature, T, °F
Location	State	Temperature, T, °F	3.524	5.35	.213			
			3.818	4.54	.181			
			Condenser	6.89	0.275			
			Barometer	29.32	-----			
Separator	1	1590	Location	State	Temperature, T, °F	Separator	1	1590
Nozzle inlet	2	1610				Nozzle inlet	2	1609
Nozzle inlet (degrees of superheat)	2	20				Nozzle inlet (degrees of superheat)	2	19
Nozzle discharge	-	1365	Separator	1	1590	Nozzle discharge	-	1364
Condenser inlet	4	1358	Nozzle inlet	2	1610	Condenser inlet	4	1359
Condenser outlet	5	1357	Nozzle inlet (degrees of superheat)	2	20	Condenser outlet	5	1356
			Nozzle discharge	-	1364			
			Condenser inlet	4	1358			
			Condenser outlet	5	1357			

Run 2A

Probe pressure tap position from nozzle inlet, in.	Pressure, p, in. Hg abs	Pressure ratio, p_x/p_2
Probe travel: outward		
0.128	16.83	0.999
.783	16.58	.984
1.429	15.56	.923
1.992	13.29	.789
2.322	11.15	.662
2.702	8.14	.483
2.922	6.50	.386
3.175	4.81	.285
3.424	4.01	.238
3.787	2.89	.172
Condenser	3.44	0.204
Barometer	29.27	-----

Location	State	Temperature, T, °F
Separator	1	1511
Nozzle inlet	2	1522
Nozzle inlet (degrees of superheat)	2	11
Nozzle discharge	-	1268
Condenser inlet	4	1258
Condenser outlet	5	1255

Run 2B

Probe pressure tap position from nozzle inlet, in.	Pressure, p, in. Hg abs	Pressure ratio, p_x/p_2
Probe travel: inward		
0.128	16.76	0.997
.306	16.85	1.002
.540	16.78	.998
.891	16.60	.988
1.191	16.17	.962
1.490	15.54	.917
1.723	14.55	.866
1.913	13.65	.812
2.067	12.77	.760
2.231	11.65	.693
2.388	10.60	.631
2.512	9.58	.570
2.702	7.79	.463
2.942	6.01	.358
3.265	4.31	.256
3.542	3.67	.218
3.797	2.90	.173
Condenser	3.46	0.206
Barometer	29.23	-----

Location	State	Temperature, T, °F
Separator	1	1514
Nozzle inlet	2	1523
Nozzle inlet (degrees of superheat)	2	9
Nozzle discharge	-	1270
Condenser inlet	4	1261
Condenser outlet	5	1258

Run 2C

Probe pressure tap position from nozzle inlet, in.	Pressure, p, in. Hg abs	Pressure ratio, p_x/p_2
Probe travel: outward		
0.717	16.80	0.987
1.168	16.23	.954
1.378	15.81	.929
1.737	14.70	.864
1.968	13.58	.798
2.241	11.77	.692
2.459	10.33	.607
2.628	8.71	.512
2.841	7.12	.418
3.097	5.29	.311
3.273	4.43	.260
3.442	4.12	.242
3.624	3.48	.204
3.797	3.00	.176
Condenser	3.49	0.205
Barometer	29.20	-----

Location	State	Temperature, T, °F
Separator	1	1515
Nozzle inlet	2	1523
Nozzle inlet (degrees of superheat)	2	8
Nozzle discharge	-	1271
Condenser inlet	4	1261
Condenser outlet	5	1256

Run 2D

Probe pressure tap position from nozzle inlet, in.	Pressure, p, in. Hg abs	Pressure ratio, p_x/p_2
Probe travel: inward		
0.358	17.00	0.994
.760	16.75	.980
1.021	16.40	.959
1.588	15.03	.879
2.031	12.89	.754
2.361	10.74	.628
2.704	7.84	.458
3.195	4.62	.270
3.791	2.99	.175
Condenser	3.69	0.216
Barometer	29.15	-----

Location	State	Temperature, T, °F
Separator	1	1515
Nozzle inlet	2	1523
Nozzle inlet (degrees of superheat)	2	8
Nozzle discharge	-	1270
Condenser inlet	4	1260
Condenser outlet	5	1256

TABLE III. - Concluded. AXIAL PRESSURE DATA (SODIUM VAPOR)

Run 3A			Run 3B			Run 4A			Run 4B		
Probe pressure tap position from nozzle inlet, in.	Pressure, p, in. Hg abs	Pressure ratio, p_x/p_2	Probe pressure tap position from nozzle inlet, in.	Pressure, p, in. Hg abs	Pressure ratio, p_x/p_2	Probe pressure tap position from nozzle inlet, in.	Pressure, p, in. Hg abs	Pressure ratio, p_x/p_2	Probe pressure tap position from nozzle inlet, in.	Pressure, p, in. Hg abs	Pressure ratio, p_x/p_2
Probe travel: inward			Probe travel: outward			Probe travel: inward			Probe travel: outward		
0.130	8.46	1.001	0.155	8.44	0.999	0.129	28.50	1.000	0.129	28.59	1.000
.305	8.42	.996	.410	8.42	.996	.432	28.37	.995	.510	28.41	.993
.505	8.44	.999	.865	8.35	.988	.686	28.17	.988	.930	27.99	.979
.770	8.46	1.001	1.141	8.15	.964	.963	27.80	.975	1.350	26.89	.940
1.280	7.98	.944	1.464	7.79	.922	1.214	27.17	.953	1.616	25.69	.898
1.589	7.66	.906	1.735	7.37	.872	1.444	26.37	.925	1.937	23.13	.809
1.857	6.93	.820	2.032	6.58	.779	1.663	24.82	.871	2.128	21.11	.738
2.114	6.23	.737	2.198	5.90	.698	1.858	23.51	.825	2.359	18.62	.651
2.256	5.65	.669	2.503	4.99	.591	2.044	21.75	.763	2.517	16.69	.584
2.392	5.23	.619	2.688	4.08	.483	2.298	18.85	.661	2.697	13.57	.474
2.594	4.44	.525	2.853	3.41	.404	2.734	12.85	.451	2.927	10.76	.376
2.956	3.02	.357	3.121	2.55	.302	2.937	9.85	.346	3.087	8.95	.313
3.281	2.12	.251	3.402	2.15	.254	3.345	6.37	.224	3.285	7.10	.248
3.559	1.80	.213	3.472	2.06	.244	3.570	5.80	.204	3.455	6.42	.224
3.787	1.48	.175	3.670	1.65	.195	3.793	4.81	.169	3.676	5.78	.202
Condenser	1.65	0.195	3.802	1.47	.174	Condenser	6.59	0.231	3.793	4.91	.172
Barometer	29.16	-----	Condenser	1.63	0.193	Barometer	29.22	-----	Condenser	6.59	0.230
			Barometer	29.16	-----				Barometer	29.28	-----
Location	State	Temperature, T, °F	Location	State	Temperature, T, °F	Location	State	Temperature, T, °F	Location	State	Temperature T, °F
Separator	1	1403	Separator	1	1404	Separator	1	1611	Separator	1	1611
Nozzle inlet	2	1442	Nozzle inlet	2	1444	Nozzle inlet	2	1624	Nozzle inlet	2	1621
Nozzle inlet (degrees of superheat)	2	39	Nozzle inlet (degrees of superheat)	2	40	Nozzle inlet (degrees of superheat)	2	13	Nozzle inlet (degrees of superheat)	2	10
Nozzle discharge	-	1198	Nozzle discharge	-	1200	Nozzle discharge	-	1365	Nozzle discharge	-	1365
Condenser inlet	4	1163	Condenser inlet	4	1163	Condenser inlet	4	1357	Condenser inlet	4	1357
Condenser outlet	5	1157	Condenser outlet	5	1159	Condenser outlet	5	1355	Condenser outlet	5	1355

2/7/25

"The National Aeronautics and Space Administration . . . shall . . . provide for the widest practical appropriate dissemination of information concerning its activities and the results thereof . . . objectives being the expansion of human knowledge of phenomena in the atmosphere and space."

—National Aeronautics and Space Act of 1958

NASA SCIENTIFIC AND TECHNICAL PUBLICATIONS

TECHNICAL REPORTS: Scientific and technical information considered important, complete, and a lasting contribution to existing knowledge.

TECHNICAL NOTES: Information less broad in scope but nevertheless of importance as a contribution to existing knowledge.

TECHNICAL MEMORANDUMS: Information receiving limited distribution because of preliminary data, security classification, or other reasons.

CONTRACTOR REPORTS: Technical information generated in connection with a NASA contract or grant and released under NASA auspices.

TECHNICAL TRANSLATIONS: Information published in a foreign language considered to merit NASA distribution in English.

TECHNICAL REPRINTS: Information derived from NASA activities and initially published in the form of journal articles or meeting papers.

SPECIAL PUBLICATIONS: Information derived from or of value to NASA activities but not necessarily reporting the results of individual NASA-programmed scientific efforts. Publications include conference proceedings, monographs, data compilations, handbooks, sourcebooks, and special bibliographies.

Details on the availability of these publications may be obtained from:

SCIENTIFIC AND TECHNICAL INFORMATION DIVISION

NATIONAL AERONAUTICS AND SPACE ADMINISTRATION

Washington, D.C. 20546